Statistical mechanics of the disjoining pressure of a planar film

J. R. Henderson
School of Physics and Astronomy, University of Leeds, Leeds LS2 9JT, United Kingdom
(Received 28 July 2005; published 11 November 2005)

The physics of wetting transitions (stability of fluid films adsorbed at planar substrates) is reassessed in the context of the original theory of wetting known as Frumkin-Derjaguin theory [A. Frumkin, Zh. Fiz. Khim. **12**, 337 (1938)]. In particular, the Russian School classify wetting phenomena in terms of the mean-field disjoining pressure. The integral of the mean-field disjoining pressure, with respect to film thickness, defines the interface potential accessible from density-functional theory (DFT). For wall-fluid models (substrate defined as an external field), the exact disjoining pressure of an adsorbed film can be expressed as a one-body sum rule. One of the aims of this work is to verify the internal consistency of the statistical thermodynamics of Frumkin-Derjaguin theory, by direct evaluation of the disjoining pressure sum rule, using DFT. For short-range models, the form of the interface potential (and hence disjoining pressure) is directly obtainable from liquid-state asymptotics. The second aim of this work is to verify from DFT that for standard short-range models there are three qualitatively different regimes, arising from competition between the correlation lengths predicted by asymptotic theory. A variety of related issues are also considered, including (i) crossover between the various regimes, (ii) incorporation of capillary-wave fluctuations (beyond mean-field), and (iii) qualitative changes induced by power-law dispersion interactions and the related prediction of two-stage wetting.

DOI: 10.1103/PhysRevE.72.051602 PACS number(s): 68.08.Bc, 68.15.+e, 68.03.Cd

I. INTRODUCTION

The exposure of a surface, for example a planar solid substrate, to a gas or liquid mixture invariably leads to adsorption of some of the fluid molecules onto the substrate surface. If this adsorption is significant, then the phenomenon is termed *wetting*. Complete wetting denotes the equilibrium growth of a macroscopically thick film at a semi-infinite planar substrate. Conversely, when a thick film placed on a substrate is thermodynamically metastable or unstable, one has partial wetting. Wetting phenomena are ubiquitous in the physical world. Essentially, every system that is capable of displaying two-phase coexistence will yield some class of wetting phenomena when placed in contact with a substrate, and both natural and technological processes are often significantly affected by wetting properties such as flotation, cleaning, painting, spraying, printing, drying, adhesion, lubrication.

Thermodynamic transitions between partial and complete wetting are examples of interfacial phase transitions. In generality we can consider the substrate to be a phase S in equilibrium with a bulk phase B, with any tendency to wetting consisting of the formation of an incipient phase of film F at the interface between S and B. Complete wetting, if it exists, must occur at two-phase coexistence between B and a macroscopic phase of F. The basic wetting phase diagram therefore consists of three thermodynamic fields, two of which (say, temperature T and film chemical potential μ) define the bulk phase diagram for coexistence between B and F while the third is some interfacial field ϵ_W that quantifies the affinity of film molecules for physical adsorption onto the surface (typically ϵ_W would denote or be some measure of a potential energy of attraction at the minimum in the interaction between a film molecule and the substrate). The important order parameter is the adsorption Γ or equivalently the film thickness ℓ, which is conjugate to the field μ. For a given temperature and substrate, the presence and nature of any interfacial wetting transition would show up in a plot of μ versus ℓ (known as an adsorption isotherm) or alternatively in a plot of the interfacial free energy (surface tension γ_{SB}) versus $1/\ell$. Repeating this process for all temperatures at which bulk BF coexistence arises and for a variety of ϵ_W values appropriate to physically relevant substrates (for example, spanning hydrophobic to hydrophilic substrates) would generate a wetting phase diagram. From such a diagram one could read off the presence and stability of film formation F at an interface between phase B placed in contact with any substrate S, governed by the existence of bulk or incipient BF coexistence. It should also be stressed that interfacial geometry alters the nature of the wetting phase diagram; for example, complete wetting is suppressed on the outside of curved substrates, but enhanced within wedge-shaped geometries (filling). In porous media, wetting phenomena are often superseded by capillary condensation (the shift in BF coexistence at finite pore width).

The physics of wetting as a class of interfacial phase transitions has a longer and more distinguished history than has sometimes been appreciated. Recently, we have seen the 200th anniversary of Young's equation [1]

$$\gamma_{LV} \cos\theta = \gamma_{SV} - \gamma_{SL} \tag{1}$$

that expresses mechanical stability in the plane of a flat rigid substrate that has had a drop of excess liquid placed on it. Outside the nanoscopic range of the direct influence of the substrate field, the drop possesses a shape defined by the contact angle θ. The liquid L and vapor V phases are at, or rather arbitrarily close to, bulk two-phase coexistence, and so $\theta=0$ corresponds to complete wetting. A wetting transition at liquid-vapor coexistence corresponds to a continuous change of θ from a finite value (partial wetting) to zero. If the rate of change of $\cos\theta$ changes discontinuously at the wetting tran-

sition, then the transition is first-order, i.e., $\gamma_{SV} \sim \cos\theta$ is the thermodynamic potential, or free energy, that controls this transition. If a series of different substrates were used to generate a change of behavior from partial wetting to complete wetting, then one would be inducing a wetting transition through variation of the field ϵ_W. In recent decades, a well-controlled experimental method for carrying out such a procedure has become available due to self-assembled monolayers [2]. Earlier work had been based on inducing wetting transitions at liquid-fluid interfaces, using temperature or the adsorption of another component to change the effective ϵ_W [3]. An even earlier procedure, still in wide use in industrial laboratories, is to vary the adsorbed fluid within a homologous (or carefully selected) series, while keeping the substrate fixed [4]. Since the wetting transition is controlled by the relative value of ϵ_W to the fluid-fluid attractive interaction strength, this procedure effectively alters ϵ_W without the need for surface chemistry [5].

The statistical thermodynamics of wetting transitions was founded almost 70 years ago by Frumkin [6] and combined with the concept of the *disjoining pressure* introduced even earlier by Derjaguin in the same context [7] and in the context of adsorption in porous media [8,9]. The Frumkin-Derjaguin theory of wetting can be regarded as the direct generalization of van der Waals's molecular theory of bulk phase transitions to interfacial phase transitions. This seminal work by the Russian School was used as the thermodynamic basis of the famous analysis of Dzyaloshinskii, Lifshitz, and Pitaevskii (DLP), who used a generalized version of Lifshitz theory to directly calculate the dispersion interaction contribution to the disjoining pressure and hence allow for explicit implementation of the Frumkin-Derjaguin statistical-thermodynamic definition of wetting transitions [10,11]. Unfortunately, the significance of wetting physics was not widely appreciated until 1977, with the independent work of Cahn [12] and Ebner and Saam [13], by which time the relevance of Frumkin-Derjaguin theory had largely been forgotten outside of the colloid and interface science community [14].

One purpose of this work is to emphasize the relevance of Frumkin-Derjaguin theory to our modern understanding of wetting transitions (Sec. II). Section III uses classical density-functional theory (DFT [13,15]) to directly calculate the disjoining pressure and thus enable us to confirm the physics of Frumkin-Derjaguin theory, at least in mean field. The second main purpose of this paper is to use DFT data to reassess the asymptotic analysis of the interface potential (the negative of the integral with respect to film thickness of the disjoining pressure) that generates phenomenological theories of wetting based on interface Hamiltonians [16,17]. Interestingly, a key component of the interface potential arises from structural (oscillatory) correlations that were also identified by a Russian group [18–20] and then largely ignored (but see [21]). For finite-range interaction models, the asymptotic analysis of fluid correlations has been carried out explicitly [21–23] and so can be applied to generate the form of the interface potential for direct comparison with DFT. The final section (Sec. IV) considers implications and generalizations of the statistical-thermodynamic route to wetting. For example, one can implement a simple version of the linear renormalization-group (LRG) approach [24] to directly renormalize the disjoining pressure, thereby incorporating capillary-wave fluctuations (at least outside of the strong fluctuation regime of critical wetting). Even without including fluctuations, the variety of contrasting correlation lengths that arise from the asymptotic analysis lead to interesting crossover effects. Ironically, one conclusion is that perhaps the only general aspect of the physics of wetting that is not well-understood in this context concerns the incorporation of dispersion interactions, as originally highlighted by a strong warning from DLP. In essence, it is not easy to consistently include power-law correlations in the same context as an asymptotic analysis of correlations induced by short-range forces.

II. DISJOINING PRESSURE

Frumkin's seminal paper in 1938 was directly concerned with the adhesion of bubbles to surfaces, modeled as a film of fluid at a substrate-gas interface [6]. Of crucial concern to this subject is the stability of the fluid film as a function of its thickness. To avoid excessive generality, let us hereafter refer to Frumkin's analysis with language appropriate to the adsorption of a liquid film at a solid-gas interface, as is readily treated with DFT and directly relevant to Young's equation. The term saturation will then denote that the gas phase would be in thermodynamic equilibrium with a macroscopic amount of liquid (i.e., the system is at bulk liquid-vapor coexistence but nucleation of bulk liquid has not taken place). We shall also implicitly assume that oversaturated gas can exist in the absence of bulk liquid, whenever required to enable the system to traverse a van der Waals loop within, for example, an adsorption isotherm.

Frumkin basis his analysis on the thermodynamic free energy of the liquid film; i.e., the interfacial excess Grand potential of the adsorbed phase, per unit surface area. Let us write this free energy, or surface tension, as γ_{SV}, which is especially appropriate to DFT (where the solid is modeled as an external field). This free energy can be regarded as a function purely of the thermodynamic fields that define the all-field phase diagram of wetting phenomena, i.e., $\gamma_{SV}(T,\mu,\epsilon_W)$. By restricting consideration to specific isotherms involving a specified substrate, one can suppress the field variables T and ϵ_W [this is the meaning of the partial derivatives appearing in Eqs. (4)–(8) below]. The order parameter conjugate to the field μ is the adsorption

$$\int_0^\infty dz[\rho(z)-\rho] \equiv \Delta\rho\ell. \tag{2}$$

Here, the notation on the left side is appropriate to a planar wall-fluid model, with the plane of infinite wall-fluid potential energy lying at $z=0$. The density profile $\rho(z)$ is the number density of adsorbed fluid at a distance z from the wall. The right side of Eq. (2) introduces an effective film thickness ℓ (at least for films thicker than a molecular size); $\Delta\rho \equiv \rho_L - \rho_V$ is a constant defined by the coexisting densities at saturation (i.e., at $\mu=\mu_{\rm sat}$). A transformation from the field μ to the order parameter ℓ is just the usual transformation be-

tween the Grand ensemble and the canonical ensemble,

$$\gamma_{SV}(\mu) = f(\ell) - \mu\Delta\rho\ell, \tag{3}$$

where $f(\ell)$ denotes the interfacial excess Helmholtz free energy per unit area. Accordingly, the above statistical thermodynamics yields the second law of thermodynamics in two equivalent forms,

$$\partial\gamma_{SV}(\mu) = -\Delta\rho\ell\,\partial\mu, \tag{4}$$

$$\partial f(\ell) = \mu\Delta\rho\,\partial\ell. \tag{5}$$

Frumkin-Derjaguin theory is typically expressed via the introduction of an interface potential $V(\ell)$ and the negative of its derivative, the disjoining pressure $\Pi(\ell)$, corresponding to a fixed chemical potential μ_o,

$$V(\ell;\mu_o) \equiv f(\ell) - \mu_o\Delta\rho\,\ell, \tag{6}$$

$$\Pi(\ell) \equiv -\frac{\partial V(\ell)}{\partial\ell}. \tag{7}$$

These functions represent the free energy of metastable or even unstable planar films, except for the value of ℓ corresponding to the absolute minimum of $V(\ell)$, where the interface potential equals the equilibrium surface tension $\gamma_{SV}(\mu_o)$. In the vicinity of a first-order interfacial phase transition, $V(\ell)$ develops a second minimum and $\Pi(\ell)$ acquires a van der Waals "loop." Direct use of these functions constitutes a mean-field theory, since at and below the upper critical dimension ($d=3$ in the case of interfacial phase transitions of short-range models [16]) $V(\ell)$ is renormalized by long-wavelength capillary-wave fluctuations away from planarity (see Sec. IV below). The Russian School summarizes the above statistical thermodynamics with the following transformation of the second law:

$$\gamma_{SV} = V + \ell\Pi, \quad \partial V = -\Pi\,\partial\ell, \quad \partial\gamma_{SV} = \ell\,\partial\Pi. \tag{8}$$

Note also that by construction

$$\Pi(\ell) = [\mu_o - \mu(\ell)]\Delta\rho, \tag{9}$$

so that one can read off the disjoining pressure, for any chosen μ_o, directly from an experimental adsorption isotherm: ℓ versus μ and hence $\mu(\ell)$. There are two equivalent approaches to applying Frumkin-Derjaguin theory in practice, for example in DFT. Frumkin emphasizes plots of the free energy versus the inverse of the order parameter, i.e., plots of γ_{SV} versus $1/\ell$. Derjaguin and DLP prefer plots of the field versus its conjugate order parameter: $\mu(\ell)$ or equivalently adsorption isotherms $\ell(\mu)$. In either case, a first-order phase transition would appear as a van der Waals loop associated with an equal-area Maxwell construction. It is a trivial matter to confirm from Eq. (8) that the equal area constructions represent equality of chemical potential (or Π) and equality of Grand potential (or V) at thermodynamic equilibrium, respectively [25]. In the absence of first-order phase transitions, every chosen value of $\mu_o < \mu_{\rm sat}$ corresponds exclusively to an equilibrium system $[\ell_o = \ell(\mu = \mu_o)]$.

In the following section, I shall use DFT to provide an explicit demonstration of Frumkin-Derjaguin theory applied to first-order wetting transitions. Being a mean-field theory, DFT is well-suited to this task, although some numerical issues do arise that require careful attention. Why then was the early work of the Russian School not widely used in previous DFT studies of wetting phenomena? The answer to this question lies partly in the lack of appreciation that Frumkin-Derjaguin theory was actually being invoked. In addition, the concept of a disjoining pressure applied to a planar semi-infinite film did not appear to be nearly as straightforward as when applied to the adsorption of fluids in porous media. In the latter case, the width of the pore acts as an additional thermodynamic field whose conjugate order parameter is the disjoining pressure. It is much more daunting to grasp the nature of the physical process that controls this pressure in the context of wetting phenomena, as one imagines the thickness of adsorbed films varying through metastable and unstable thermodynamic states. For the present author, the required understanding has come through the consideration of fluids adsorbed on structured substrates, in particular within linear triangular wedges [26–28]. This statistical mechanics equates Derjaguin's disjoining pressure with the force per unit area exerted on the adsorbed fluid by the substrate; for a planar wall-fluid model defined by an external field $v^{\rm ext}(z)$ this yields the obvious formula (see also [29])

$$\Pi(\ell) = -\int_{-\infty}^{\infty} dz\big[\rho(z;\ell) - \rho^{\infty}(z)\big]v^{\rm ext\prime}(z), \tag{10}$$

where $\rho(z;\ell)$ is the density profile of an adsorbed film of thickness ℓ and $\rho^{\infty}(z)$ denotes the limit of a macroscopically thick film; i.e., the wall-liquid density profile [30]. Of course, this force is precisely what DLP calculated from generalized Lifshitz theory, or rather they calculated the dispersion interaction contribution to it. In 1978, Derjaguin and Churaev recognized that the direct use of statistical mechanics by DLP to evaluate the disjoining pressure of an adsorbed film was an important conceptual advance [31]. The Russian School expressed this force in terms of the normal component of a pressure tensor [32], which by Newton's third law must generate a result equivalent to Eq. (10). Of special interest to wetting phenomena is the recent proof that the integral of the disjoining pressure along a substrate containing an adsorbed drop generates an expression of force balance normal to the substrate that must be the direct analogue of Young's equation (1). Namely [26],

$$\gamma_{LV}\sin\theta = -\int_{-}^{+} dx\Pi(x), \tag{11}$$

where the variable x runs along the substrate over an interval $-$, $+$ spanning the three-phase contact line formed by the liquid-vapor interface at its intersection with the planar substrate. In fact, this exact sum rule can be directly related to Frumkin-Derjaguin theory applied to the spreading pressure [27]. Modern DFT is fully consistent with sum rules of the class (10), which can be reexpressed in terms of the gradient of the one-body direct correlation function [33]. Thus, given also that a specific DFT is defined exclusively by a choice of free-energy functional and hence interface potential, it fol-

lows that one should expect DFT to be completely consistent with the entire statistical-thermodynamic structure of Frumkin-Derjaguin theory.

III. DENSITY-FUNCTIONAL THEORY AND ASYMPTOTIC ANALYSIS

Classical DFT can be used to carry out a Frumkin-Derjaguin analysis of wetting transitions in any of the three equivalent statistical-thermodynamic approaches summarized in Eq. (8), provided one has access to metastable and unstable regions of phase space. In particular, DFT provides the minimum free-energy (i.e., solid-vapor surface tensions) and adsorption (film thickness) as a function of chemical potential. A plot of minimum free-energy versus inverse film thickness would yield a Frumkin analysis (analogous to a pressure versus volume isotherm of a bulk phase transition), while plotting chemical potential versus film thickness would be a Derjaguin analysis (analogous to a chemical potential versus density isotherm of a bulk transition). In practice, the overwhelmingly popular choice has been to calculate the interface potential as a function of film thickness (analogous to a Landau theory of a bulk phase transition). Experimentally, a Frumkin analysis is most appropriate to wetting at fluid substrates, since solid-fluid surface tensions are rarely accessible. In contrast, Derjaguin stressed that chemical potential differences can be expressed as pressure differences, which are experimentally accessible at solid-fluid interfaces [8]. Due to sum rule (10), one should be able to use DFT to carry out a Derjaguin analysis directly in terms of the disjoining pressure $\Pi(\ell)$, which could then be compared with the derivative of $V(\ell)$ obtained from the free-energy functional. This self-consistency test will be our first important task. We shall then ask what consequences must follow for the physical interpretation of an interface potential.

The interface potential $V(\ell)$ is the surface excess Grand potential per unit area of an adsorbed film of thickness ℓ, as defined directly by the Grand potential of a density-functional theory. For a specific choice of chemical potential μ_o there is a unique value of ℓ for which this potential is the free energy of an equilibrium film, except at a first-order wetting transition where there will be two equal minima. At any other value of the chemical potential this thickness must correspond to a nonequilibrium fluctuation away from the minimum. The route to calculating $V(\ell;\mu_o)$ from DFT is therefore to partially minimize the surface excess Grand potential for a range of constrained film thicknesses; i.e., subject to a constraint of fixed adsorption. This constraint ensures that the interface potential is a mean-field free energy, because in the absence of the constraint the film would develop long-wavelength capillary-wave fluctuations away from planar symmetry. For the same reason, the disjoining pressure $\Pi(\ell)$ must also be a mean-field quantity. Of course, there exist renormalization-group methods for including fluctuations, to which I shall refer in the discussion. In practice, it has been noted that standard Picard iteration methods applied to the minimization of the Grand potential essentially automatically yield the value of $V(\ell)$ associated with the film thickness of the initial trial density profile $\rho(z)$; i.e., the local

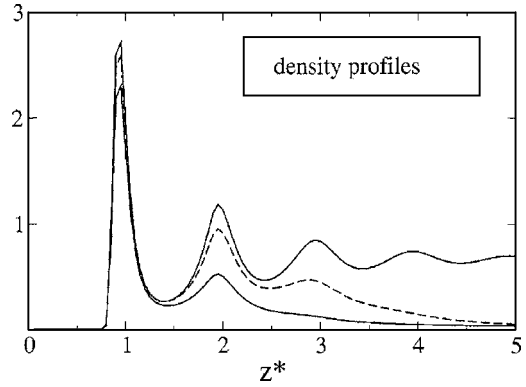

FIG. 1. Density profiles $\rho(z^*)\sigma^3$ where $z^* \equiv z/\sigma$ and σ is the fluid-fluid molecular diameter defined by a cut and shifted (at $r=2.5\sigma$) 12-6 potential. The substrate wall is composed of three layers of cut and shifted (at $z=2.5\sigma$) 10-4 wall; the plane of infinite repulsive wall-fluid energy lies at $z=0$. The data belong to a first-order wetting transition at bulk liquid-vapor coexistence for a temperature of $T=0.80T_c$. The solid profiles belong to complete wetting and to the thin molecular film that is in coexistence with complete wetting, respectively. The dashed profile corresponds to a planar film lying at the free-energy maximum (the transition state). The profiles were obtained from mean-field density-functional theory; see text.

structure of the density profile is rapidly minimized while in contrast the film thickness drifts slowly toward the global minimum [34]. Figure 1 shows examples of density profiles for a system at bulk liquid-vapor coexistence undergoing a first-order wetting transition. The interface potential is plotted in Fig. 2. The choice of DFT is representative of a functional designed to represent a short-range model, in this example, three solid layers of cut and shifted 10-4 potential make up the substrate and the fluid is cut and shifted 12-6

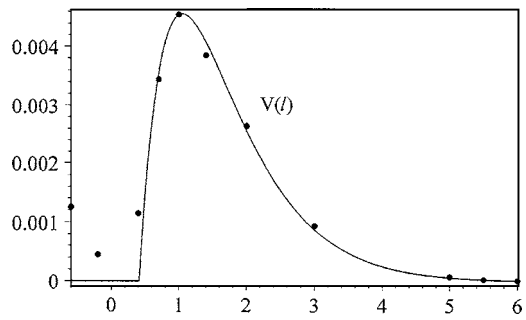

FIG. 2. Mean-field interface potential $V(\ell/\sigma)\sigma^2/k_BT$ as a function of the thickness of adsorbed planar films ℓ/σ, for a system lying close to a first-order wetting transition at bulk liquid-vapor coexistence; the same system whose density profiles are plotted in Fig. 1. The symbols denote DFT data; in particular, the point lying closest to the origin is the true thin-film minimum (see the lowest profile in Fig. 1) while the highest point lies at the free-energy maximum (the dashed profile in Fig. 1). The remaining DFT data were obtained by enforcing a crossing constraint, to allow for numerical convergence of films that would otherwise be metastable/unstable; see text. The curve shows the prediction of liquid state asymptotics, fitted only to the position and height of the maximum; $0.1101\exp(-1.42\ell/\sigma)-0.1258\exp(-1.74\ell/\sigma)$.

[35]. The three density profiles correspond to the molecularly thin-film minimum and completely wet film (full curves) together with the transition state lying at the maximum in the interface potential (dashed curve). In fact, these three states are the only ones that can be essentially fully equilibrated with Picard iteration, without suffering significant global drift toward the nearest minima in $V(\ell)$. Typically, one ignores this drift by choosing a small number of iterations when filling in the remainder of the interface potential (not drawn in Fig. 2). However, the rapidly varying nature of the integrand on the right side of sum rule (10) prevents this simple approach from being applicable to direct calculation of the disjoining pressure; the result is a highly distorted disjoining pressure. Instead, one must use a constraint to fix the film thickness while the free energy is minimized to a sufficient level. The filled circles in Fig. 2 denote results obtained with a simple crossing constraint [36]; i.e., the position of the liquid-vapor interface is identified with the largest value of z at which the density profile of a suitably chosen initial choice crosses the average of the liquid and vapor densities and this single value is kept fixed throughout the minimization. This procedure is adequate to achieve sufficient minimization without serious distortion, but could of course be improved on if desired [37]. The thin-film minimum is the point closest to the origin, which is fully converged in the absence of the crossing constraint (yielding the lowest density profile in Fig. 1). This value lies slightly above the thick-film limiting value (used to define the zero of the interface potential), showing that for this choice of T, ϵ_W, and numerical grid, the system lies just beyond the wetting transition from partial to complete; it is of course not possible to sit exactly on the transition. The highest point (corresponding to the dashed profile in Fig. 1) lies at the maximum free energy and also converged without requiring a crossing constraint. The remaining points show DFT data that converged only when the constraint was applied (apart from the three thickest films which are only included to illustrate the asymptotic theory discussed below). It would be straightforward to repeat these constrained minimizations for many different choices of constrained film thickness and then plot a continuous curve for $V(\ell)$. However, nothing more can be learned from this time-consuming exercise. Instead, let us attempt to identify the overall shape of the interface potential from physics; in particular, we can analytically derive the full line shown in Fig. 2 from asymptotic theory discussed below. First, however, let us use the crossing constraint DFT to verify the internal consistency of Frumkin-Derjaguin theory.

The points plotted in Fig. 3 show values of the disjoining pressure calculated directly from its definition (10). From the relation (7) it follows that the disjoining pressure should be zero wherever the interface potential passes through a stationary point. All three zeros (including the large thickness limit) correspond correctly to the stationary points in Fig. 2 and in addition these are the values which converge without the crossing constraint. Elsewhere, the points have been converged with the same crossing constraint used to generate Fig. 2. The direct numerical error is smaller than the size of the symbols. The finite grid size induces error of the order of the symbol size, due to the rapidly varying nature of the integrand on the right of Eq. (10); in fact, to obtain the true zero of the disjoining pressure one must subtract off an essentially constant error arising from the finite grid (that is readily obtained from the thick-film limit). In addition, the simple choice of crossing constraint involves a somewhat larger error, arising from local drift of metastable and unstable states toward the nearest minimum, which are not fully suppressed by the constraint (see above). Thus, the agreement between Fig. 2 and 3, expressed by the relation (7), is a completely convincing demonstration of the internal statistical mechanical consistency of Frumkin-Derjaguin theory of first-order wetting transitions. In particular, the full line in Fig. 3 shows the analytic asymptotic theory described below; the straight lines are just a guide to the eye. Note also that because the system lies very close to a first-order wetting transition, the disjoining pressure displays an equal area Maxwell construction, between the first zero and the thick-film limit. Applying this statistical thermodynamics to the partial wetting regime at saturation, the equivalent construction reduces to probably the most well-known expression from Frumkin-Derjaguin theory [8],

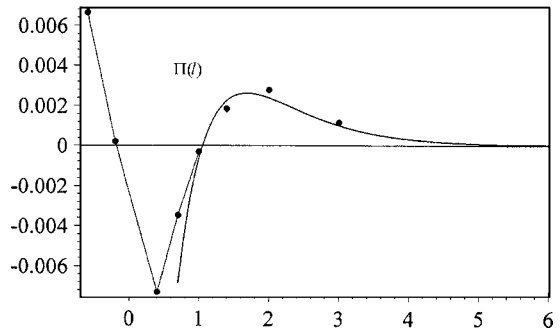

FIG. 3. Disjoining potential $\Pi(\ell/\sigma)\sigma^3/k_BT$ for the same system whose density profiles and interface potential are plotted in Figs. 1 and 2, respectively. The symbols were obtained from a direct calculation of sum rule (10) using DFT. The straight lines are plotted to guide the eye; note the approximate equal area construction (between the first zero in the disjoining pressure and the thick-film limit) as is appropriate to a system lying close to a first-order wetting transition. The full curve is the prediction of liquid-state asymptotics fitted to the interface potential, i.e., minus the derivative of the curve in Fig. 2.

$$-\int_{\ell_o}^{\infty} d\ell \Pi(\ell) = V(\infty) - V(\ell) = \gamma_{LV}(1 - \cos\theta), \qquad (12)$$

where ℓ_o denotes the equilibrium solid-vapor interface (the molecularly thin film) and the final equality has introduced Young's equation (1) for the contact angle θ. An equivalent expression is [38]

$$\ell_o \int_0^{1/\ell_o} d\frac{1}{\ell} \gamma_{SV}(\ell) = V(\ell_o) \equiv \gamma_{SV}. \qquad (13)$$

These two results express the statistical thermodynamics for quasistatically thinning a macroscopically thick film of excess liquid down to its equilibrium thickness.

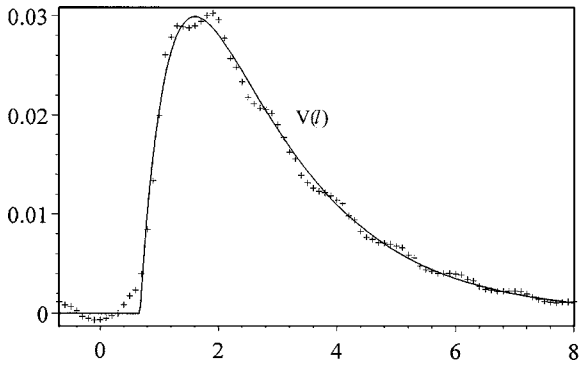

FIG. 4. Mean-field interface potential $V(\ell/\sigma)\sigma^2/k_BT_c$ as a function of the thickness of adsorbed planar films ℓ/σ, for a system lying close to a first-order wetting transition at bulk liquid-vapor coexistence; from DFT of square-well fluid at a square-well wall (here σ denotes the repulsive core of the square wells). The temperature at which this first-order wetting transition is occurring is $T=0.64T_c$, which is much lower than the system shown in Figs. 1–3. As a result, the long-range oscillatory decay is now apparent at medium range, as a weak modulation of the interface potential. The curve shows the prediction of liquid state asymptotics, fitted only to the position and height of the maximum (leaving out the damped oscillation which could be trivially added if desired); $0.105\exp(-0.56\ell/\sigma)-0.25\exp(-1.85\ell/\sigma)$.

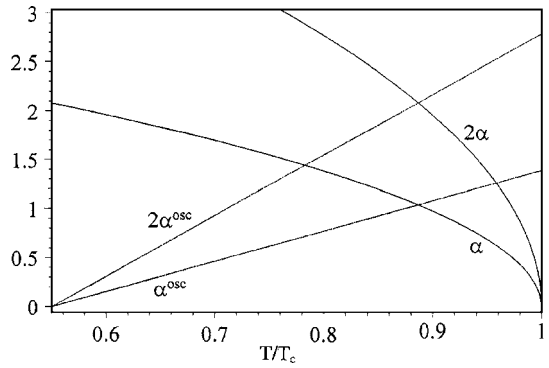

FIG. 5. Inverse correlation lengths from liquid state asymptotics, for saturated liquid as a function of temperature along the liquid-vapor coexistence curve. The data were generated from the standard mean-field model of square-well fluid (the unit of length for the ordinate is taken to be the repulsive core diameter of the square well), but the qualitative behavior is believed to be universal for all short-range models. This asymptotics applies equally to the radial distribution function of the liquid, the liquid tail of the vapor-liquid profile, wall-liquid density profiles, or interface potentials and disjoining pressures; see text. For example, the leading-order decay of the density profile away from a planar wall is of the form $\rho(z/\sigma)-\rho_L=a\exp(-\alpha z/\sigma)+b\exp(-\alpha^{\rm osc}z/\sigma)\cos(kz+\phi)+$h.o.t., where k lies close to $2\pi/\sigma$, ϕ is a nonuniversal phase, and a and b are nonuniversal amplitudes. The inverse decay lengths for $[\rho(z/\sigma)-\rho_L]^2$ contributions are also plotted, since typically they are well-separated from the plethora of higher-order terms needed to define the shortest-range structure. In particular, note the long-range nature of the $2\alpha^{\rm osc}$ decay in the vicinity of the triple point. In contrast, the 2α pure monotonic decay is only of significance close to the liquid-vapor critical point.

Figures 1–3 present data from the same functional at a saturation temperature of about 80% of the liquid-vapor critical temperature T_c. In contrast, Fig. 4 shows the interface potential of a system lying much closer to the triple point; $T/T_c=0.64$ [39]. The symbols plotted in Fig. 4 are standard DFT data obtained without imposing a crossing constraint (thus the sum-rule route to the disjoining pressure is not available here—except for thick films where the oscillatory nature was confirmed directly). At first sight, the overall shape of the interface potential, which clearly lies very close to a first-order wetting transition, appears to be of the same form as Fig. 2. However, the observant reader will have noticed the clear oscillations that modulate the basic shape; in fact, in mean field at least this wetting transition can only be described as pseudowetting [21]. To understand the origin of this qualitative difference in the interface potential, which in turn will influence the overall shape, we can turn to the theory of liquid-state asymptotics [22,23]. One can argue that all structural decay into a given bulk fluid, such as observed in wall-fluid density profiles and the fluid radial-distribution function, are controlled by the same set of correlation lengths. These in turn must also control the asymptotic behavior of fluid mediated correlations, such as the solvation force of a planar pore or, the case of direct interest here, the disjoining pressure and interface potential of a planar film [21]. Figure 5 shows the behavior of the largest correlation lengths, along the entire liquid-vapor coexistence curve of saturated liquid, that control the leading-order (asymptotic) structure of a short-range model. The figure is quantitatively accurate for the standard square-well model, but is qualitatively relevant to all short-range models of the liquid state. The curve labeled α denotes the inverse bulk correlation length defined by mean-field theory. Namely, the long-range decay with distance z of any structural property contains a pure exponential decay proportional to $\exp(-\alpha z)$. This class of asymptotics dominates in the region of the liquid-vapor critical point. In contrast, exponentially damped oscillatory decay, familiar from typical radial-distribution functions or wall-liquid density profiles, dominates at lower temperatures and typically diverges somewhere around the true equilibrium transition to crystal. In Fig. 5, the line labeled $\alpha^{\rm osc}$ denotes the inverse decay length of this exponential damping. The wavelength of these decaying oscillations is, of course, close to the repulsive molecular diameter of the model, as evidenced in Fig. 4. Formally, these lengths are defined by a pole analysis in the complex plane (at points where the bulk liquid structure factor diverges). Density-functional theory automatically satisfies this asymptotic theory; i.e., the numerical procedures calculate the appropriate integrals over the direct correlation function as part of the minimization procedure, whenever the density profile structure has reached an asymptotic (or even intermediate) region of decay. For example, from analyzing the decay of the wall-liquid profile in Fig. 1 one can read off the value of $\alpha^{\rm osc}$ appropriate to the cut and shifted 12-6 functional; $\alpha^{\rm osc}=0.87$ at $T/T_c=0.80$. At this relatively high temperature, the amplitude of these oscillations is too small to be observed in the interface potential and is only just observable on the liquid side of the liquid-vapor profile far from the interface. Accordingly, one can extract the pure exponential decay

length from the medium-range behavior of the liquid-vapor profile; $\alpha=1.42$ at $T/T_c=0.80$. The crossover point $\alpha=\alpha^{\rm osc}$ just below $T/T_c=0.9$ in Fig. 5, defines the intersection of the Fisher-Widom line with the liquid-vapor coexistence curve [22,23]. At temperatures above this value, the longest-range decay into saturated liquid is pure monotonic, while below this temperature it is damped oscillatory.

The curves labeled $2\alpha^{\rm osc}$ and 2α plotted in Fig. 5 are also directly relevant to the shape of the interface potential. One can regard the interface potential, or disjoining pressure, as arising from the interference between the liquid structure that is induced at either side of the adsorbed film, by the substrate wall and by the liquid-vapor interface, respectively. Note that asymptotic theory implies that these two components decay with identical correlation lengths and (for the oscillatory term) the same wavelength. Thus, one expects $(\delta\rho)^2$ contributions, with inverse decay lengths of $2\alpha^{\rm osc}$ and 2α, to be present in the interface potential and disjoining pressure. One could envisage extending this series indefinitely, but for a typical short-range model only those contributions plotted in Fig. 5 are significantly separated from the higher-order behavior that controls the short-range structure to enable them to be clearly separated out. In an important but not widely appreciated contribution to our understanding of wetting, Mikheev and Chernov have argued that near the triple point the leading-order decay of an interface potential must be given by the $2\alpha^{\rm osc}$ contribution [18–20]. We can illustrate the nature of this physics from Fig. 4 and 5. First, from Fig. 5 it is obvious that near the triple point the pure exponential term is much shorter-range ($2\alpha^{\rm osc}\ll\alpha$). Then from Fig. 4 we can appreciate that the linear oscillatory contribution (decay length $\alpha^{\rm osc}$) can only modulate the overall structure of the interface potential. Furthermore its amplitude is quite weak, presumably reflecting the natural tendency of an oscillatory contribution to be washed out by fluctuations (in fact, if long-wavelength capillary-wave contributions were included beyond mean-field DFT, then these oscillations would be of negligible amplitude [21]). In contrast, the second-order term is expected to be nonoscillatory (some average over the squares of oscillations) and to be dominant at intermediate range in the interface potential.

The above physics, extracted from analytic asymptotic theory, demands a specific form for the intermediate and long-range behavior of the interface potential (or disjoining pressure). In particular, at a first-order wetting transition the long-range decay must be repulsive and the intermediate decay (toward the thin-film minimum) must be attractive. Thus, if we ignore the linear oscillatory modulation, the interface potential in Fig. 4, corresponding to $T/T_c=0.64$, must be of the form

$$V(\ell) = b\exp(-2\alpha^{\rm osc}\ell) - a\exp(-\alpha\ell) + \text{h.o.t.}, \qquad (14)$$

where a and b are positive amplitudes and "higher-order terms" (h.o.t.) denotes the short-range structure that must be present in the form of a positive repulsion to complete the thin-film minimum. The physics implies that Eq. (14) should dominate from less than a molecular diameter away from the first minimum out until only the linear oscillatory term is left. We can use the DFT data in Fig. 4 to directly confirm this physics. In particular, we can insert the decay lengths as plotted in Fig. 5 and determine the amplitudes a and b by fixing the position and height of the maximum in the interface potential. The solid curve plotted in Fig. 4 shows the outcome of this analytic fit. The result is strong confirmation that Eq. (14) captures the physics of a mean-field interface potential, for temperatures sufficiently close to the triple point. However, Fig. 5 implies that the significance of the two terms controlling the interface potential will have swapped over when the temperature has increased to $T/T_c=0.8$. That is, the interface potential plotted in Fig. 2 must be of the form

$$V(\ell) = a\exp(-\alpha\ell) - b\exp(-2\alpha^{\rm osc}\ell) + \text{h.o.t.}, \qquad (15)$$

where a and b are again defined to be positive. Inserting the decay lengths for the cut and shifted 12-6 model, quoted earlier, and evaluating the amplitudes by fitting just the position and height of the maximum, yields the full curve plotted in Fig. 2. The negative derivative of this curve is plotted in Fig. 3, to illustrate that analytic asymptotics is equally useful in explaining the nature of the disjoining pressure obtained directly from sum rule (10). From Fig. 5 we can note that it is only at temperatures above the Fisher-Widom point around $T/T_c=0.9$ that the interface potential will be given by the standard mean-field expression typically applied to wetting phenomena of short-range models [16,17],

$$V(\ell) = a\exp(-\alpha\ell) - c\exp(-2\alpha\ell) + \text{h.o.t.} \qquad (16)$$

The explicit comparison between DFT and analytic asymptotic theory, presented above, is a gratifying demonstration that one understands the physics of the mean-field interface potential of wetting films. Since we also found that the statistical mechanical definition of the disjoining pressure is fully consistent with the statistical thermodynamics that defines the interface potential, we can also claim to have confirmed the physics of the disjoining pressure route to interfacial wetting transitions. An important caveat is that the Russian School can justly claim to have published the essentials of this wetting physics as long ago as 1938. Notwithstanding, we are still left with a variety of "loose ends," some of which are discussed in the final section below.

IV. DISCUSSION

This paper has used DFT and liquid-state asymptotics to explore the underlying physics that determines mean-field interface potentials and disjoining pressures of liquid films adsorbed at planar walls. For such models, one can write down the sum rule (10), which identifies the exact disjoining pressure as the ensemble-averaged force per unit area that the wall imparts to the film molecules. This result could also be expressed in terms of the normal component of the fluid pressure tensor acting on the wall (essentially by Newton's third law), which is in fact the identification on which DLP founded their theory of thick film stability [10,11,32]. This statistical mechanics generalizes beyond planar symmetry, where the wall-fluid route is particularly powerful (the use of pressure tensors beyond planar symmetry is fraught with difficulties). In particular, the statistical thermodynamics of flu-

ids adsorbed in a wedge (or at an edge) has been expressed in terms of moments of the disjoining pressure as a function of distance from the wedge (edge) apex [26–28].

By applying liquid-state asymptotics to mean-field DFT, we have observed that the qualitative structure of the interface potential changes along the liquid-vapor coexistence curve. There are three regimes of behavior. From the triple point up to about half-way to the critical temperature, the interface potential displays a relatively strong first-order wetting transition, in which the barrier is dominated by a competition between a positive medium-range exponential decay with a correlation length $1/2\alpha^{\rm osc}$ and a negative shorter-range exponential contribution with correlation length $1/\alpha$. This basic shape is modulated by a damped oscillatory term (correlation length $1/\alpha^{\rm osc}$) that only dominates for very thick films (pseudowetting) and beyond mean field would be essentially washed out by capillary-wave fluctuations. The next regime extends up to where the Fisher-Widom line crosses liquid-vapor coexistence. The interface potential continues to show first-order wetting, but now the medium-range decay is a positive pure exponential decay and the $2\alpha^{\rm osc}$ term kicks in at shorter range to favor a molecularly thin film. Formally, the linear damped-oscillatory term is still present at longest range, but the amplitude is now so small as to be numerically insignificant even in strict mean field. Only for temperatures close to the critical point is the interface potential dominated by the pure exponential decay terms (α and 2α). At first, in this final regime, DFT continues to yield first-order wetting [a and c are positive in Eq. (16)], but eventually before the critical point is reached c changes sign at the wetting transition (now the wetting transition is continuous and occurs at the temperature at which $a=0$). To observe all of this behavior with DFT, one simply needs to vary the strength of the wall-fluid attraction ϵ_W to generate a wetting transition curve in the T, ϵ_W plane [40]. The special point on this wetting curve at which $a=c=0$ is the tricritical point where the wetting transition changes from first-order to continuous. Locating the tricritical point numerically by trying to identify where the first-order barrier in the interface potential becomes zero is not easy [41]. One can now see that part of the problem is that the barriers at low and medium temperatures belong to qualitatively different regimes, so that an attempt at extrapolation from temperatures where the barrier is high is problematic; see, for example, [33].

The assiduous reader will be enquiring as to the nature of the two crossover boundaries between the three regimes. Both crossovers maintain the first-order nature of the wetting transition and yet the amplitudes of the two competing terms must change sign at the transition. This can only happen if the amplitudes are formally infinite at the crossover points, as worked out in detail by Aukrust and Hauge for a simplified model functional [41]. We can map the first crossover point onto their analysis by considering the interface potential

$$V(\ell) = a\exp(-\alpha\ell) + b\exp(-\beta\ell) + c\exp(-2\alpha\ell), \tag{17}$$

where c is a finite positive amplitude (this final term represents all the shortest-range contributions to the interface potential) and to maintain the shape appropriate to a first-order wetting transition we must insist that for all states a and b possess opposite signs. The crossover occurs at $\alpha=\beta$. The conditions for first-order wetting can be taken to be $V(0)=0$, $V'(0)=0$, $V'(\ell_m)=0$; the first two conditions simply set the thin-film minimum to lie at the origin $\ell=0$ while ℓ_m denotes the film thickness at the free-energy maximum (from DFT, ℓ_m is around one or two molecular diameters). Inserting these three conditions into Eq. (17), one obtains

$$a = -\frac{c(2\alpha-\beta)}{\alpha-\beta}, \quad b = \frac{c\alpha}{\alpha-\beta}, \tag{18}$$

$$V(\ell_m) = c\exp(-\alpha\ell_m)[1-\exp(-\alpha\ell_m)]\frac{(2\alpha-\beta)}{\beta}. \tag{19}$$

Note that at crossover, a and b change sign by passing simultaneously through infinity, from opposite directions, but that the interface potential varies smoothly with an almost imperceptible signature of the crossover. Namely, very close to crossover, $(\beta-\alpha)\ell \ll 1$ is consistent with large values of ℓ and one might just be able to detect that the interface potential now decays at long range as $c(\alpha\ell-1)\exp(-\alpha\ell)$, rather than a pure exponential. Close to a crossover boundary, one cannot attach physical meaning to the amplitudes a and b obtained by fitting DFT data for an interface potential to a series of exponentials, rather at crossover all physical significance is transfered to the short-range amplitude c. The decay lengths are determined by liquid-state asymptotics, but the amplitudes can only be obtained from the full functional. Since the wetting transition curve constitutes a strong mathematical constraint on the relationship between the amplitudes, one must not attach an overly physical meaning to them.

The approach to complete wetting and continuous wetting transitions of short-range models is qualitatively affected by capillary-wave fluctuations in dimensions $d \leqslant 3$. The standard approach to including long-wavelength fluctuations is to extend the interface potential to include a square-gradient term (whose coefficient is the liquid-vapor surface tension) and then apply a renormalization-group method. At the upper critical dimension $d=3$, linear renormalization (LRG) is sufficient and is equivalent to first smearing (convoluting) $V(\ell)$ with a Gaussian and then applying standard mean-field theory, apart from the strong fluctuation regime of critical wetting [21,24]. There are two diverging correlation lengths associated with continuous wetting transitions, for long-wavelength capillary-wave correlations induced along the interface and for their contribution to the interfacial roughness, respectively,

$$\xi_{\|}^2 \equiv \gamma_{LV}/(\partial^2\bar{V}(\ell)/\partial\ell^2)_{\ell_o}, \tag{20}$$

$$\xi_{\perp}^2 \equiv \frac{k_BT}{2\pi\gamma_{LV}}\ln(\Lambda\xi_{\|}), \quad d=3, \tag{21}$$

where $\bar{V}$ denotes the renormalized interface potential, k_B is Boltzmann's constant, and Λ is a short-wavelength cutoff (of the order of the inverse of a molecular diameter). The per-

pendicular correlation length is the same length that controls the extent of Gaussian renormalization. Thus, one can start with the mean-field interface potential and apply a simple Gaussian smearing to extract renormalized wetting phenomena. To date, this physics has only been consistently carried out in the high-temperature regime (16); see the discussion in Ref. [21]. The same Gaussian renormalization applies to the mean-field density profile [42]. Thus, one could alternatively apply linear renormalization directly to the statistical mechanical definition of the disjoining pressure (10). The singular contribution to the disjoining pressure must be contained within the quantity

$$\int_0^\ell dz[\rho_L - \tilde{\rho}(z;\ell)]v^{\text{ext}'}(z)f(z). \tag{22}$$

Here, $\tilde{\rho}(z;\ell)$ denotes the liquid tail of the liquid-vapor profile, interpolated to the substrate without distortion from the substrate field and then renormalized by smearing with a Gaussian. The function $f(z)$ is a short-range damping function that is needed to take account of the direct effect of the substrate field on the fluctuations; clearly, $f(z)$ contains the factor $\exp[-v^{\text{ext}}(z)/k_BT]$. For a short-range external field, it is then clear that the singular part of the disjoining pressure must be proportional to the difference between $\tilde{\rho}(0)$ and its limiting value ρ_L at complete wetting. Let us denote this difference as $\delta\tilde{\rho}(\ell)$, where the origin has been shifted to the position of the liquid-vapor interface and so the substrate is located a distance ℓ away, inside the liquid tail of the liquid-vapor profile. The renormalized asymptotics of the disjoining pressure for a short-range model is therefore of the form $\bar{\Pi}(\ell) \sim \delta\tilde{\rho}(\ell)$ [43]. That this precise class of renormalization together with standard capillary-wave theory (20) and (21) recovers LRG predictions for the nature of continuous wetting transitions has been explicitly demonstrated elsewhere [44,45]. This form is to be expected from mean-field liquid-state asymptotics, since identical damped-oscillatory and pure-exponential decay appear on the liquid side of the density profile of the liquid-vapor interface as found in the interface potential of a wetting film of the same liquid (i.e., identical apart from amplitudes). Linear renormalization preserves this equivalence. In this context, it is interesting to note that Mikheev and Weeks have shown that the statistical mechanical sum rules that highlight the presence of capillary-wave contributions can actually be rewritten as pair-force correlations defined in terms of a fluctuating disjoining pressure [the instantaneous version of Eq. (10)] [29].

Power-law interactions shift the upper critical dimension for continuous transitions to lie below $d=3$ [46], so that mean-field DFT is then predicted to be qualitatively correct for interfacial critical phenomena in the physical world (due to the ubiquitous presence of dispersion interactions). However, this is not the same mean-field theory presented in Sec. III. The Russian School was fully aware of the relevance of dispersion interactions to the thick-film regime of wetting phenomena and interfacial density profiles. Frumkin includes a derivation of the leading-order contribution of dispersion interactions to the disjoining pressure [6]. One can confirm this result directly from the statistical mechanical definition (10),

$$\Pi(\ell) = -\int_{-\infty}^{\ell} dz[\rho(z;\ell) - \rho^{\infty}(z)]v_{\text{SR}}^{\text{ext}'}(z) + \Delta\rho\int_{\ell}^{\infty} dz v_{\text{LR}}^{\text{ext}'}(z) + \text{h.o.t.}, \tag{23}$$

$$= a\,\delta\rho(\ell) - \Delta\rho v_{\text{LR}}^{\text{ext}}(\ell) + \text{h.o.t.} \tag{24}$$

Here, the substrate field has been divided into a short-range component plus long-range power-law terms. When the dispersion interactions between the substrate and the film are integrated over the semi-infinite space occupied by substrate, then $v_{\text{LR}}^{\text{ext}}(\ell)$ is seen to be a power series with a leading-order term varying as ℓ^{-3} (ignoring retardation). The short-range substrate term in Eq. (24) dominates at the substrate wall, but nevertheless generates an identical power series (apart from amplitude a) because the long-range decay of the liquid tail of the liquid-vapor interface toward saturated liquid is defined by the same class of integral over power-law interactions (in this case fluid-fluid interactions) [47]. The amplitudes of the power-law terms in the interface potential have been calculated analytically for standard models [48]. Of course, Lifshitz theory, as derived by DLP [10,11], is the formally exact direct route to the dispersion interaction contribution to the interface potential and hence disjoining pressure. However, none of these approaches contains a recipe for making a clear distinction between power-law contributions and the remainder of the mean-field interface potential. In fact, DLP appear to highlight this dilemma by stating that Frumkin's seminal contribution is derived "without explicitly distinguishing between a(d)sorptive and wetting films" [10]. There appear to have been two contrasting responses to this dilemma among the wider community. In materials and colloid science, the usual approach is to apply Lifshitz theory down to molecular dimensions, thereby subsuming short-range interactions into effective Hamaker constants, in direct violation of the instructions supplied by the originators of the theory. The other response is to follow the Russian School and restrict Lifshitz theory to the description of mesoscopically thick wetting films only [49]. Let us now consider these two approaches in turn.

The main difficulty with the first approach is that one is lost when trying to identify a short-range interaction contribution to the interface potential, i.e., the analogues of Figs. 2 and 4. The distinction between contributions to long-range (power-law) and short-range (exponential) terms is irretrievably blurred. Ideally, one would like to be able to apply asymptotic theory and identify two distinct sets of terms to include in the interface potential. However, deep mathematical problems arise at the outset. In particular, the presence of a power-law interaction, no matter how weak, qualitatively alters Fig. 5 by completely removing pure exponential decay (there is no pole on the imaginary axis in the presence of a power-law interaction [50]). In contrast, the damped oscillatory decay is almost unaffected by the presence of power-law interactions, for physically relevant values of the Hamaker

constants. Thus, one might conclude that the class of interface potential that applies in the physical world is of the form (cf. [50])

$$V(\ell) = a\ell^{-2} + b\ell^{-3} + c\exp(-2\alpha^{\mathrm{osc}}\ell) + \text{h.o.t.} \qquad (25)$$

The main caveat with this interfacial potential is its applicability to the near-critical region, where in the absence of power-law interactions the asymptotics arises from a diverging correlation length α^{-1}, even in mean field.

The alternative approach is to follow the advice of DLP and accept that power-law interactions break down below some mesoscopic range, via a mechanism that has still not been quantified to date. Even the language appears unhelpfully mysterious. Some would restrict "dispersion interactions" to fluctuations in the quantum electrodynamics of macroscopic amounts of matter. The Russian School prefers the title "van der Waals forces," but the "short-range" intermolecular attractions of a cut and shifted 12-6 model of molecular matter do not sit easily with the restriction to mesoscopic length scales [51]. Interestingly, the clear view of DLP as to the length scale at which dispersion interactions influence the interface potential is supported by modern experiments on the wetting of water by simple oils (remember that water hates oil but not vice versa). Adsorption isotherms have been measured that display two-stage wetting; at some temperature, the system leaves the usual partial wetting regime by forming a thick but not macroscopic film of adsorbed oil. At a higher temperature, the oil film then undergoes a continuous transition to complete wetting [52]. Furthermore, this final transition coincides with the leading-order Hamaker constant passing through zero; cf. Eq. (25). Frumkin himself reports early experimental data that are tentatively identified with the first stage of this scenario: (i) oleic acid electrolyte solutions on mercury and (ii) methyl alcohol on charcoal [6]. In this approach, one might hope to be able to understand wetting phenomena via a complete separation of length scales. The power-law interactions could then only influence wetting at mesoscopic thicknesses and short-range models would be sufficient to extract the wetting behavior of molecularly thin films.

In summary, Frumkin-Derjaguin theory and its more or less independent rediscovery 40 years later constitute a powerful theory of interfacial wetting phenomena that has been convincingly confirmed by modern DFT. A variety of length scales control different aspects of the physics of wetting, which when combined with fluctuations create such a complex set of phenomena that significant areas remain unexplored to date. Ironically, the one regime believed to represent the physical world, whose study was the focus of the Russian School, is perhaps the least understood. Essentially, how can one include dispersion interactions without losing control over the short-range contributions that should dominate wetting by molecularly thin films?

ACKNOWLEDGMENTS

I am especially grateful to Roland Roth for providing a complete translation into English of the German translation of Frumkin's 1938 paper [6], which was then checked against the original Russian by Ania Maciolek. I also thank Simon Dixon for a partial translation of key sections of the original Russian.

[1] T. Young, Philos. Trans. R. Soc. **95**, 65 (1805).
[2] D. J. Durian and C. Franck, Phys. Rev. Lett. **59**, 555 (1987); **59**, 1492 (1987).
[3] M. R. Moldover and J. W. Schmidt, Physica D **12**, 351 (1984).
[4] H. W. Fox and W. A. Zisman, J. Colloid Sci. **5**, 514 (1950).
[5] D. E. Sullivan, J. Chem. Phys. **74**, 2604 (1981).
[6] A. Frumkin, Zh. Fiz. Khim. **12**, 337 (1938); translated into German in Acta Physicochim. URSS, **9**, 313 (1938).
[7] As reviewed by Frumkin [6].
[8] B. V. Derjaguin and N. V. Churaev, in *Fluid Interfacial Phenomena*, edited by C. A. Croxton (Wiley, Chichester, 1986), Chap. 15 and references therein.
[9] N. V. Churaev, Adv. Colloid Interface Sci. **104**, xv (2003); see the introduction to this issue devoted to B. V. Derjaguin, and references therein.
[10] I. E. Dzyaloshinskii, E. M. Lifshitz, and L. P. Pitaevskii, Sov. Phys. JETP **37**, 161 (1960).
[11] I. E. Dzyaloshinskii, E. M. Lifshitz, and L. P. Pitaevskii, Adv. Phys. **10**, 165 (1961).
[12] J. W. Cahn, J. Chem. Phys. **66**, 3667 (1977).
[13] C. Ebner and W. F. Saam, Phys. Rev. Lett. **38**, 1486 (1977).
[14] See, for example, footnote 6 of Ref. [13]. For an exception that did stress the importance of the Russian School to our understanding of wetting phenomena, see G. F. Teletzke, L. E. Scriven, and H. T. Davis, J. Colloid Interface Sci. **87**, 550 (1982). Of course, a large part of the excitement generated in 1977 was due to Cahn's important (albeit flawed) argument which implied that by increasing the temperature of any partially wet system, while maintaining bulk fluid-fluid coexistence, one must cross a wetting transition, regardless of the nature of the substrate, before reaching the fluid-fluid critical point. The ubiquitous presence of wetting transitions was thus emphasized.
[15] R. Evans, Adv. Phys. **28**, 143 (1979).
[16] R. Lipowsky, D. M. Kroll, and R. K. P. Zia, Phys. Rev. B **27**, 4499 (1983).
[17] E. Brézin, B. I. Halperin, and S. Leibler, J. Phys. (Paris) **44**, 775 (1983).
[18] L. V. Mikheev and A. A. Chernov, Sov. Phys. JETP **65**, 971 (1987).
[19] A. A. Chernov and L. V. Mikheev, Phys. Rev. Lett. **60**, 2488 (1988).
[20] A. A. Chernov and L. V. Mikheev, Physica A **157**, 1042 (1989).
[21] J. R. Henderson, Phys. Rev. E **50**, 4836 (1994).
[22] R. Evans, J. R. Henderson, D. C. Hoyle, A. O. Parry, and Z. A. Sabeur, Mol. Phys. **80**, 755 (1993).
[23] R. Evans, R. J. F. Leote de Carvalho, J. R. Henderson, and D.

C. Hoyle, J. Chem. Phys. **100**, 591 (1994).
[24] D. S. Fisher and D. A. Huse, Phys. Rev. B **32**, 247 (1985).
[25] Frumkin provides diagrammatic examples of wetting phenomena in the context of this statistical thermodynamics. His Fig. 1 shows a complete wetting and a partial wetting regime (partial wetting is referred to as incomplete wetting). Figure 2 is used to define a first-order wetting transition, together with the appropriate Maxwell construction. That Frumkin understands this to be a first-order wetting transition is abundantly clear from the text and the summary, but in the figure Frumkin does not equate the surface tensions of the two films in coexistence. From discussion later in the text, it appears that Frumkin has done this in order to be able to apply his analysis to bubble adhesion close to but not quite at complete wetting (at complete wetting, the bubble would be detached). Accordingly, if one reads the text carefully and notes that Frumkin draws the Maxwell construction as a horizontal tie-line, it can be concluded that he expects readers to understand that equilibrium wetting requires the two free energies at the ends of the tie-line to be equal. His Fig. 3 shows an example of an interfacial phase transition associated with the nearby presence of first-order wetting, but this time between two films of differing finite thicknesses (and here the two surface tensions at either end of the Maxwell construction are correctly equated). Frumkin describes this transition in identical terms to its current name: the thin-thick transition. Early experimental data are available to enable Frumkin to tentatively suggest physical relevance to both these interfacial phase transitions. DLP prefer to describe Frumkin's and Derjaguin's work in terms of adsorption isotherms [10,11]. They give five examples of different classes of wetting phenomena, including a clear example of the thin-thick transition and its Maxwell construction, lying off saturation. Partial wetting and complete wetting isotherms are also displayed, but the first-order wetting transition at saturation is relegated to a footnote. This type of analysis was later reinvented by J. G. Dash [Phys. Rev. B **15**, 3136 (1977)], who introduced the labels type I, II, and III to denote adsorption isotherms appropriate to complete wetting, partial wetting, and nonwetting, respectively (the last two classes are really the same, labeled *c* by DLP, while complete wetting is labeled *b* in DLP). The analysis of DLP is more complicated because their results are presented in terms of long-range dispersion interactions alone, without explicitly including the short-range contributions that DLP note are required to describe the molecularly thin-film region.
[26] J. R. Henderson, Phys. Rev. E **69**, 061613 (2004).
[27] J. R. Henderson, Mol. Simul. **31**, 435 (2005).
[28] J. R. Henderson, Mol. Phys. **103**, 2839 (2005).
[29] L. V. Mikheev and J. D. Weeks, Physica A **177**, 495 (1991).
[30] Eq. (10) assumes the system to be at saturation $\mu_o=\mu_{\rm sat}$. Otherwise, $\rho^{\infty}(z)$ would need to be replaced by the density profile of the equilibrium thin film ℓ_o. Alternatively, one could simply subtract $(\mu_{\rm sat}-\mu_o)\Delta\rho$ from the right side of Eq. (10); see Eq. (9).
[31] B. V. Derjaguin and N. V. Churaev, J. Colloid Interface Sci. **66**, 389 (1978).
[32] For a recent formulation applied to arbitrary geometry, see A. I. Rusanov and A. K. Shchekin, Mol. Phys. **103**, 2911 (2005).
[33] F. van Swol and J. R. Henderson, Phys. Rev. A **40**, 2567 (1989).
[34] P. Tarazona and R. Evans, Mol. Phys. **48**, 799 (1983).
[35] J. R. Henderson, P. Tarazona, F. van Swol, and E. Velasco, J. Chem. Phys. **96**, 4633 (1992), and references therein.
[36] M. E. Fisher and A. J. Jin, Phys. Rev. B **44**, 1430 (1991).
[37] A single crossing constraint is not sufficient to prevent localized drift of the profile and so equilibrated density profiles lying in between those displayed in Fig. 1 possess an unsightly glitch at the crossing point. Nevertheless, this procedure does lead to a minimized density profile that can be used to evaluate sum rule (10), since the glitch does not contribute to the short-range integrand. For films in the region of the thin film minimum, one might query the suitability of using Eq. (2) to replace the adsorption with an effective film thickness. In fact, in all the data presented here, the variable ℓ is actually defined from the position of the liquid-vapor dividing surface of the initial trial profile. One can readily check that switching to the definition (2) will only affect the shape of the thin-film minimum (not its position nor the rest of the interface potential); since the crossing constraint does not completely prevent drift, this alternative choice appears to be more narrow than is physically sensible. Finally, to ensure a uniform standard for comparing interface potentials from different functionals and different numerical procedures, the choice of origin for ℓ has always been made to ensure that the molecularly thin-film minimum at a first-order wetting transition lies close to $\ell=0$.
[38] Note from Eq. (8) that $\gamma_{SV}=(\partial/\partial 1/\ell)(V/\ell)$.
[39] It should also be noted that the functionals are based on different models. Similarly, there are a wide variety of DFT functionals in common use. The functionals used here are based on hard-core weight functions chosen for consistency at high temperature with the hard-sphere bulk equation of state. For the attractive interactions, the functional used to generate Figs. 1–3 contains an attractive-interaction contribution that is fitted to computer simulation data for the cut and shifted 12-6 bulk equation of state [35], whereas Fig. 4 displays data obtained from a standard DFT applied to square-well fluid adsorbed at a square-well wall [21]. However, such differences are not relevant to the purposes of this paper because the interface potentials of short-range models displaying liquid-vapor coexistence are qualitatively similar. In essence, one has rough corresponding states for interfacial tensions and for the correlation lengths defining the shape of the interface potential (Fig. 5).
[40] D. E. Sullivan and M. M. Telo da Gama, in *Fluid Interfacial Phenomena*, edited by C. A. Croxton (Wiley, Chichester, 1986), Chap. 2.
[41] T. Aukrust and E. H. Hauge, Physica A **141**, 427 (1987).
[42] J. K. Percus, Faraday Symp. Chem. Soc. **16**, 23 (1981).
[43] One should be aware that for interfacial critical phenomena, an exponentially decaying substrate field is not a short-range model. Strictly, an exponential has infinite range and therefore reaches out to sense the rapidly varying part of the liquid-vapor interface. This would contribute another term of exactly the same class, apart from the different exponential decay length; cf. Eq. (24).
[44] J. R. Henderson, Mol. Phys. **59**, 1049 (1986).
[45] J. R. Henderson, Mol. Phys. **62**, 829 (1987).
[46] R. Lipowsky, Phys. Rev. Lett. **52**, 1429 (1984).
[47] For a derivation of the power-law tails of a liquid-vapor density profile in the language of DFT, see J. A. Barker and J. R.

Henderson, J. Chem. Phys. **76**, 6303 (1982).
[48] S. Dietrich, in *Phase Transitions and Critical Phenomena*, edited by C. Domb and J. Lebowitz (Academic Press, London, 1988), Vol. 12.
[49] This issue is highlighted by DLP with an estimation of a typical contact angle in the partial wetting regime obtained from dispersion interactions alone; it is as small as 0.1 degrees corresponding to a "thin"-film minimum of around 500 nm.
[50] R. J. F. Leote de Carvalho, R. Evans, D. C. Hoyle, and J. R. Henderson, J. Phys.: Condens. Matter **6**, 9275 (1994).
[51] In fact, Rowlinson has pointed out that van der Waals died before quantum mechanics and therefore had no reason to anticipate universal power-law interactions. Instead, when required for his theory of capillarity, van der Waals chose an $\exp(-\alpha r)/r$ attraction. Ironically, this general form for a fluid-mediated interaction was independently rediscovered at least twice by succeeding generations and is never referred to as a van der Waals interaction; J. S. Rowlinson, Physica A **156**, 15 (1989).
[52] N. Shahidzadeh, D. Bonn, K. Ragil, D. Broseta, and J. Meunier, Phys. Rev. Lett. **80**, 3992 (1998).